Development of a Dual Phase - Low Alloy Steel for Laser Powder Bed Fusion (LPBF)

Chris Schade, Tom Murphy, and Kerri Horvay
Hoeganaes Corporation
Cinnaminson, NJ 08077

ABSTRACT

Development of low alloy steels for laser powder bed fusion is difficult because high carbon levels are used to develop strength and hardness. These high carbon levels often lead to cracking due to the elevated levels of residual stresses caused by the transformation of the microstructure to martensite. Additionally, the layer-by-layer heating from the laser leads to a tempering of martensite producing a softer material than the equivalent wrought steels. By creating a dual phase microstructure, a steel can be developed with a range of mechanical properties that may be varied by post-printing heat treatments. The microstructure can be varied from a fully martensitic structure that exhibits high strength to a microstructure with elevated levels of ferrite leading to a steel that has high ductility. The mechanical properties and microstructures of these various heat treatments are reviewed along with potential applications including those in the automotive industry.

INTRODUCTION

The development of additive manufacturing (AM) has not come without challenges for powder manufacturers. The various platforms for additive manufacturing printers require a variety of particle size distributions which typically utilize less than 50% of the full atomized distribution. In addition, AM production volumes are limited to a small quantity of parts, because the use of AM is favored when the design of the part is intricate and cannot be produced by conventional processes. If the design is not a factor, high volume parts can be produced at lower costs by utilizing methods such as stamping, forging and even powder metallurgy processes such as press and sinter and metal injection molding (MIM). While not the dominant cost in AM, the powder portion of the total cost to manufacture is significant and has led to the adaptation of powders that are currently used in other powder parts making processes due to their inherent availability. For example, 316L stainless steel is used in conventional powder metallurgy (press and sinter), metal injection molding, as well as thermal spray applications. Therefore, powder already exists in a range of particle sizes that can be adapted for AM. For the powder producer, the best method to keep the cost of powders at a minimum is to maximize the sales of the individual particle size distributions required by the end customer.

An example of the particle size distribution from a gas atomized powder is shown in Figure 1. It shows the full distribution of a gas atomized powder and the various size ranges that can be produced from it. Typically, three different powder sizes for AM manufacturing processes can be taken from the full distribution: Metal Binder Jet (MBJ), Laser Powder Bed Fusion (LPBF), and Direct Energy Deposition (DED). The LPBF process requires a

powder in the 15–53 micrometer size range, while the MBJ process requires a finer powder for sinter-ability (in the < 25-micrometer range). The DED process utilizes powder in a 45-105 micrometer size range. These three size ranges are shown in Figure 1 and comprise nearly the whole distribution of the atomized powder and therefore each AM process utilizes one-third of the distribution. If the powder producer can find customers for all three of the AM printing techniques, then the quantity of powder can be fully utilized. If the producer can only sell one or two of the distributions (1/3 or 2/3 of the full distribution) then the cost to the customer needs to be increased due to the poor yield of the atomized material.

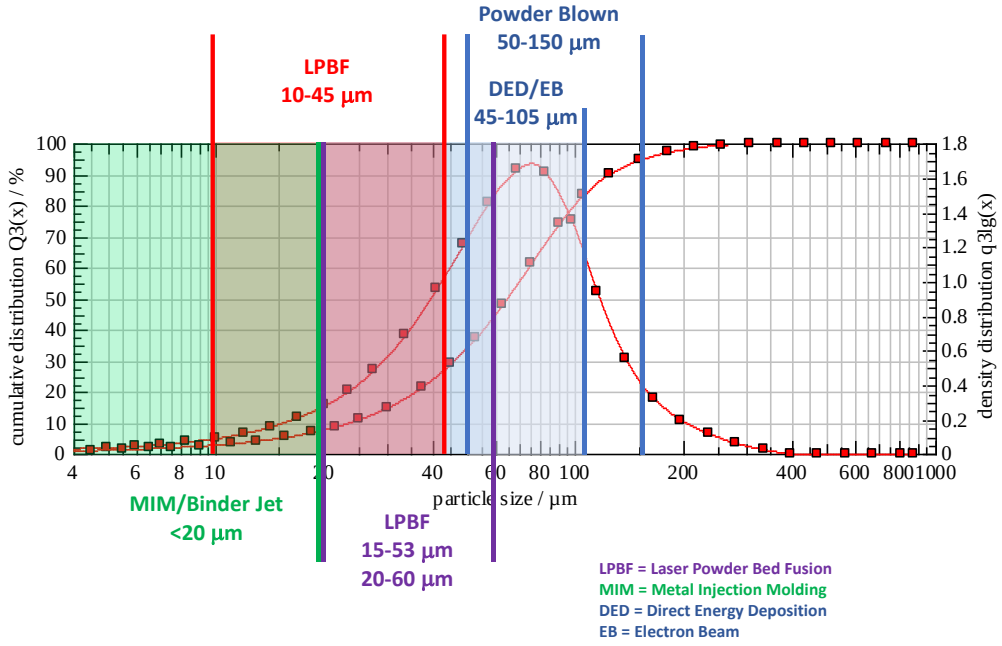

Figure 1: Powder particle size distribution of gas atomized powder depicting the various size distributions for AM processes that can be achieved from the full atomized distribution.

The second issue for powder manufacturers (and the AM parts builder) is that the distinctive design of AM parts requires properties not specifically available in the current alloys available for the conventional powder metallurgy (PM) and MIM markets. Therefore, special compositions must be designed, which typically will be designed for a specific AM manufacturing process, i.e., for MBJ, LPBF, or DED. This requires the powder producer to develop the market for the additional powder not being utilized by the specific process called for by the customer. Therefore, the price of the material can increase by two to three times due to only a portion of the full powder particle size distribution being utilized for the part. This dilemma impacts the growth of additive manufacturing as a whole and typically limits the powder selection to those powders that are already available in PM and MIM, i.e., 316L, 17-4PH, etc.[1-2] One area that has seen increased interest from both the automotive and structural parts industries is the development of low alloy steels. In the case of MBJ, the higher carbon content of these materials leads to poor sinter-ability (i.e., MIM-4605) and for LPBF/DED

processes. The higher carbon leads to stress cracks due to the fast cooling and martensitic microstructure. However, both automotive and industrial applications are growing for additive manufacturing, so the development of low alloy steels is of critical importance.

In previous work, an alloy called FSLA (Free Sintering Low Alloy) was introduced for MBJ and MIM with comparable properties to wrought DP600 (i.e., Ultimate Tensile Strength (UTS) = 600 MPa).[3-5] Wrought DP600 acquires its dual phase (DP) microstructure and mechanical properties through a combination of controlled rolling and intercritical anneal heat treatments.[6-9] In addition to DP600, there are a range of DP alloys used in conventional wrought processing that have ultimate tensile strengths ranging from 480 MPa to 1050 MPa (shown in red in Figure 2). In many cases, this is accomplished by increasing the carbon level to the same base alloy chemistry and then applying various heat treatments to optimize the mechanical properties by altering the microstructure.[10]

Unlike other low alloy steels available for additive manufacturing, the chemical composition of the FSLA alloy was originally tailored to have a mixed microstructure of approximately fifty volume percent ferrite and fifty volume percent austenite at the sintering temperatures. Work by previous authors had suggested that the increase in grain boundary area between the austenite and ferrite would increase the diffusion and lead to a higher sintered density.[11-12] This was proven to be the case as the MBJ/MIM based FSLA, which both required sintering, had superior sintered density compared with other low alloy steels such as the MIM-4605 sintered at the same temperature. The ferrite stabilizing elements (chromium, molybdenum, and silicon) were all chosen because of their hardenability characteristics. The alloy composition allowed for inter-critically annealing (heat treatment) at various temperatures in the two-phase region of austenite and ferrite. With appropriate cooling rates, the austenite will transform to martensite (and/or bainite) and a final microstructure of various levels of ferrite and martensite/bainite (the typical microstructure of dual phase steels) can be achieved. This flexibility in microstructure led to a wide range of mechanical properties for the alloy when utilized in MBJ and MIM as shown in Figure 2.

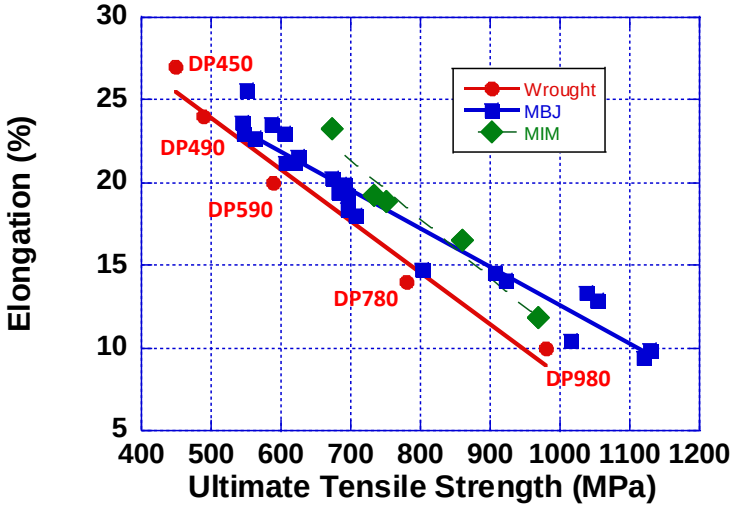

Figure 2: Mechanical properties of FSLA after different heat treatments. Includes MIM, MBJ and wrought grades of Dual Phase Steels.[1-3]

The target properties of the wrought grades of dual phase steels were consistently met by this development work as evident by Figure 2, but the ability to use the same alloy composition in LPBF is complicated by the fact that the thermal processing of a part made from LPBF (melting) is vastly different than that manufactured by MBJ or MIM (sintering). However, an alloy designed to achieve a wide range of mechanical properties by post-printing heat treatments is desirable to save on print parameter development. Therefore, this paper details the printing and heat treatments of the LPBF-FSLA to produce a wide range of ultimate tensile strength and ductility combinations without significant changes to its composition or the printing parameters. The properties will then be compared to the MIM and MBJ properties that were optimized in previous works.

EXPERIMENTAL PROCEDURE

Powders utilized in this study were air melted and gas atomized with nitrogen. Chemical analysis and powder properties are listed in Table I.

Table I: Powder properties of Air Melted- Gas Atomized FSLA. Chemical composition shown in weight percent.

	Apparent Density	Tap Density	Carbon	Sulfur	Oxygen	Nitrogen	d_{10}	d_{50}	d_{90}	Hall Flow
Material	g/cm^3	g/cm^3	wt.%	wt.%	wt.%	wt.%	Micrometers	Micrometers	Micrometers	Secs
FSLA Powder 15-53 Microns	4.31	5.26	0.12	0.007	0.03	0.010	14.0	31.0	48.4	27.8

	Cr	Si	Mo	Cu	Ni	V	Nb	Mn	Fe
Material	wt.%	wt.%	wt.%	wt.%	wt.%	wt.%	wt.%	wt.%	wt.%
FSLA Powder 15-53 Microns	1.67	1.62	1.59	0.03	0.07	0.22	0.20	0.05	Bal.

Scanning Electron Microscopy images of the powder utilized in this study are shown in Figure 3. The shape factor (the length dimension divided by the width), and the internal porosity of the powder were measured with image analysis and determined to be 0.80 and 0.09% respectively.

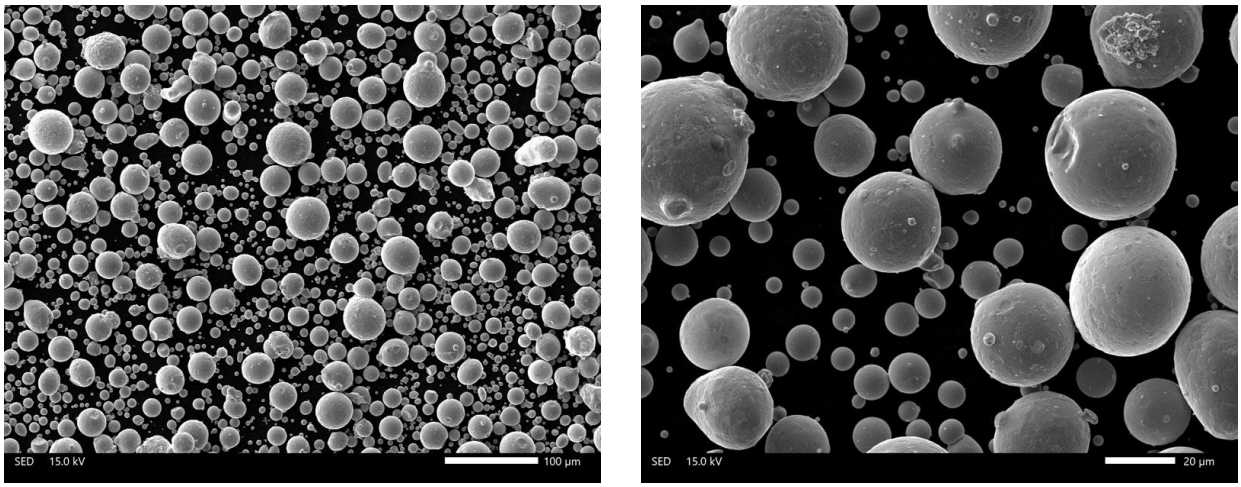

Figure 3: Scanning Electron Microscope images of the FSLA powder for LPBF.

The powder used in this study was screened from the same material (0.12 wt.% carbon) that was used in previous studies for developing the FSLA for MBJ and MIM.[1-3] The intent was to examine whether two powder distributions could be utilized from the overall atomized distribution and therefore increase the yield of usable powder.

An EOS M290 AM machine with a build volume of 250 mm by 250 mm by 325 mm was used to make the specimens for this study. A Yb fiber laser (400W) was utilized and the build chamber was filled with argon. Process settings were varied to find the optimal energy density for the material being.

Cubic samples (10 mm by 10 mm by 10 mm) were printed with a variety of settings to evaluate the porosity content produced with the material. A constant layer thickness was used for all the samples while the laser power, hatch distance and scanning speed were changed. Image analysis, following MPIF Standard Guide 69, was used to measure the porosity content of the cross-section of the cubes perpendicular to the build direction. A set of standard settings (based on the minimum porosity level acheived) was used to build the mechanical testing specimens in the Z direction for this study. Samples were cut from the build plate in the as-built condition.

For continuous heat treatment, a high temperature Abbott continuous-belt furnace was used at indicated temperatures for 30 minutes in an atmosphere of 95 vol.% nitrogen / 5 vol.% hydrogen. Forced cooling was performed in the final zone of the furnace (cooling = 1.3 ^{o}C/sec).

Batch heat treatments were performed in either a vacuum furnace or a standard box furnace heated to the indicated temperature in an atmosphere of 95 vol.% nitrogen / 5 vol.% hydrogen.

Prior to mechanical testing apparent hardness was measured on the samples. Five tensile specimens (flat dogbones/unmachined) were evaluated for each condition. The densities of the sintered steels were determined in accordance with MPIF Standard 42. Tensile testing followed MPIF Standard 10, and apparent hardness measurements were made on the tensile specimens, in accordance with MPIF Standard 43.[13]

The microstructure was revealed, and color was used to separate the transformation products with a two-step, etch/stain process. First, the microstructure was defined with a light pre-etch by immersing the sample in Vilella's Reagent (5 mL HCl + 1 g picric acid + 100 mL ethyl alcohol), rinsing with warm water, and drying with filtered compressed air. In the second step, the pre-etched sample was immersed in a freshly prepared solution of 10 g sodium metabisulphite ($Na_2S_2O_5$) in 100 mL deionized or distilled water, rinsed with warm water and alcohol, then dried with filtered compressed air.

RESULTS AND DISCUSSION

One of the unique features of the FSLA alloy is the wide range of temperatures in which the alloy can be heat treated in the two-phase region of austenite and ferrite. This is shown by the Calphad diagram in Figure 4. When heat treated at a temperature of approximately 870 ^{o}C (Point A), the microstructure of the FSLA alloy is > 90% ferrite. Conversely, when held at temperatures near 1200 ^{o}C (Point B), the microstructure is ~ 90% austenite which can transform to either

bainite or martensite depending on the cooling rate. One of the key features of dual phase steels is the ability to vary the mechanical properties by changing the levels of martensite, bainite and ferrite in the final microstructure. If a material of higher strength and hardness is required, intercritical annealing is performed at a temperature at which there is an elevated level of austenite that can transform during cooling. The cooling can also be varied including furnace cooling, gas quenching or liquid medium quenching (either oil or water). If a material with lower strength but better ductility is required, an intercritical anneal temperature favoring the formation of the softer ferrite phase is chosen. To evaluate the range of properties the FSLA alloy could exhibit, it was decided to evaluate several different heat treatments from LPBF samples that would allow for a broad range of microstructures. Each of those heat treatments are now described.

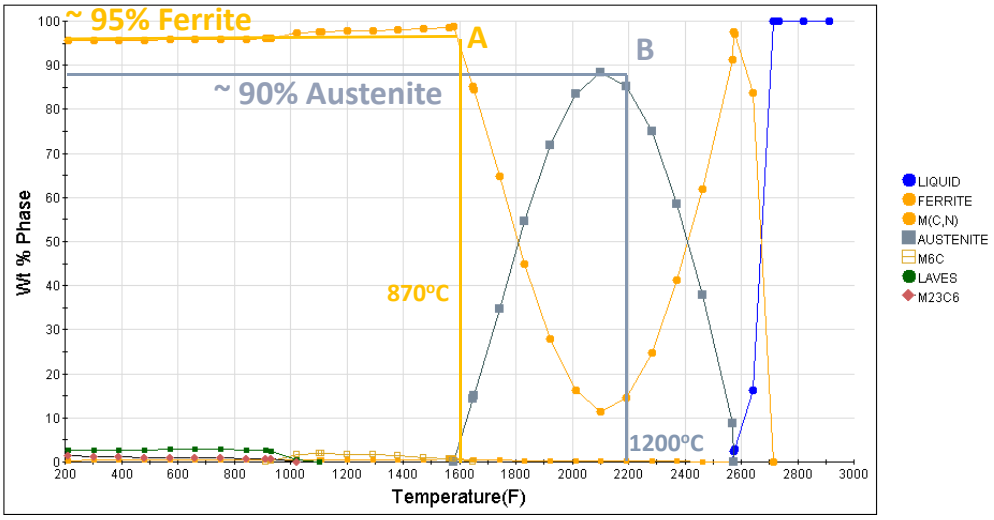

Figure 4: CALPHAD generated diagram for the phases present at various temperatures for the FSLA alloy chemical composition shown in Table I.

Heat Treatment (0)- To fully understand the alloy both microstructure and properties must be examined. Table II shows the mechanical properties of the FSLA. Heat Treatment (0) is in the as built condition. Since the FSLA contains elements such as chromium, molybdenum, and silicon that all individually impart a significant amount of hardenability to the alloy, the alloy contains transformation products that form during cooling.

Table II: Mechanical properties of FSLA LPBF (0.12% wt.% carbon) samples given different heat treatments.

Heat Treat #	Condition	UTS [MPa]	0.2%YS [MPa]	Elong [%]	Hardness [HRA]
0	As Built	720	539	< 1.0%	53
1	1200 °C 1hr / 800 °C 2hr	592	423	28.6	47
2	IA 850 °C Furnace Cool	670	400	26.5	49
3	IA 1200 °C 1 hr Gas Quench	726	517	23.7	51
4	IA 1200 °C Water Quench	925	528	17.1	56

The microstructure is shown in Figure 5 for the as built condition. There is a variation in grain size that is typical of welded structures. Since the cooling rate is slow due to the multiple passes

of the laser the microstructure consists of ferrite with coarse carbides (primarily molybdenum and niobium) located along the grain boundaries. Although the chromium, molybdenum, and silicon increase the hardenability, in general they are ferrite stabilizers, and due to the slow cooling rates, they limit the amount of transformation product that has formed. A small amount of bainite has just started to nucleate along the grain boundaries of the ferrite phases.

The ultimate tensile strength of the material exceeds 700 MPa, however due to the coarse and brittle carbides and bainite along the grain boundaries, the ductility as indicated by the tensile elongation is extremely poor. It would not be recommended that this material be used in the as built condition. As will be seen in subsequent discussions, heat treatments which refine the microstructure led to improved properties.

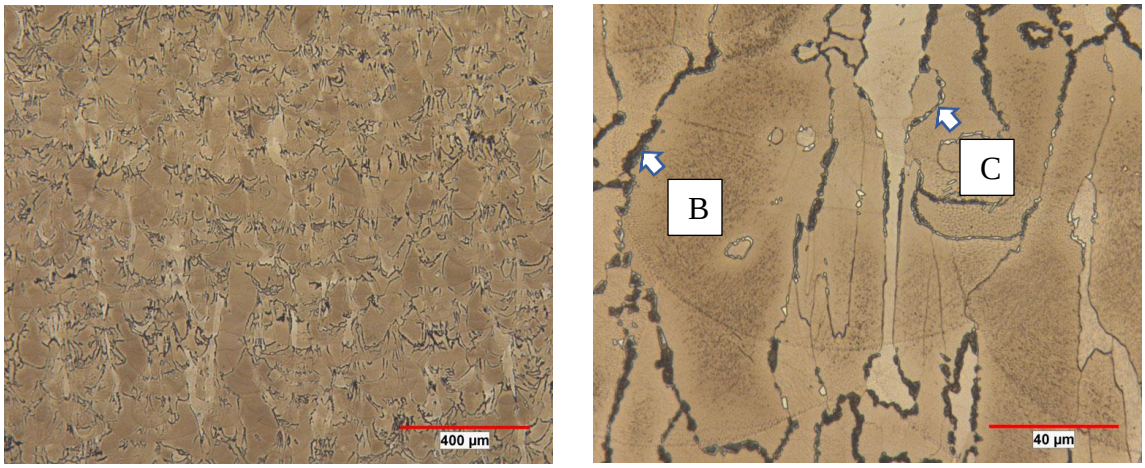

Figure 5: Optical micrographs of the FSLA in the as printed condition. Higher magnification on right shows bainite (B) and carbides (C) along grain boundaries.

Heat Treatment (1): This heat treatment was designed to provide an elevated level of ferrite in the microstructure to produce a steel with the maximum amount of ductility. The microstructure of the FSLA alloy after the printing process is a mixture of ferrite and a small quantity of bainite and carbides located along the grain boundaries (Figure 5). To maximize the ferrite from this starting microstructure, it was necessary to re-austenitize the as built samples, allowing the already transformed bainite to transform to austenite. This was followed by cooling to allow this austenite to transform to ferrite. For this reason, the samples were heated for 1 hour at 1200 ^{o}C to form austenite from the pre-existing bainite, followed by a furnace cool to an intercritical anneal temperature of 800 ^{o}C. Holding at this temperature allowed for the transformation of a high percentage of the elevated temperature austenite to ferrite. To maximize ductility, there is a necessity to balance the level of ferrite which predominates at the lower temperatures (800 ^{o}C) with the amount of carbide formation from elements like molybdenum, niobium, and vanadium. The precipitates that form from these elements were useful in creating the high strength necessary in the DP980 alloy, but hinder dislocation motion and therefore limit the ductility of the alloy at the range necessary to achieve the desired elongation values for alloys with a lower UTS strength (< 480 MPa).

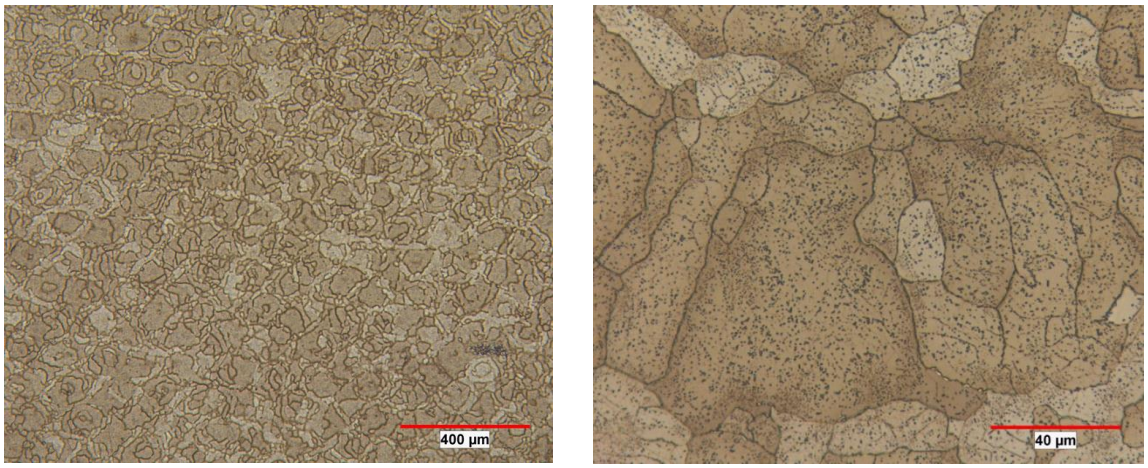

Figure 6: Optical micrographs of the FSLA alloy heat treated at 1200 ^{o}C for 1 hour then furnace cooled and held at 850 ^{o}C for 2 hours to maximize the ferrite content. Higher magnification on right shows carbides in the interior of the grains.

The microstructure in Figure 6 shows the two distinct types of ferrites, the ferrite which formed upon cooling from solidification (the lighter shade) and the ferrite formed during the intercritical anneal (darker phase). The heat treatment also includes a gas quench from the inter-critical to quickly reduce the temperature to below that at which the carbides are forming. Any reduction of carbide formation will lead to an enhancement of the ductility of the alloy. The ductility achieved by this heat treatment is significantly higher than conventional wrought dual phase alloys at a similar ultimate tensile strength.

Heat Treatment (2): This heat treatment was originally developed for the MBJ-FSLA to achieve properties close to the commercial DP600 alloy (UTS = 600 MPa, Elongation = 25% minimum). The processing conditions for this material were heating to 850 ^{o}C in a continuous furnace and then utilizing a gas quench in the last zone of the furnace to cool to room temperature. The microstructure that forms, shown in Figure 7, is like the microstructure formed in the as built condition. Here the structure is ferrite (both primary and secondary) with a small amount of transformation product that has formed on the ferrite grain boundaries (bainite). However due to the re-heating, the inhomogeneous grain structure that formed during the LPBF solidification process has been replaced by a more uniform grain structure without any indications of the original melt pools due to the laser melting. The ferrite is the predominate phase and while the structure produced by the heat treatment is like that of the as built condition, the homogenization of the grain structure and the reduced level of carbides at the grain boundaries leads to a superior ductility as measured by the elongation percentage shown in Table II.

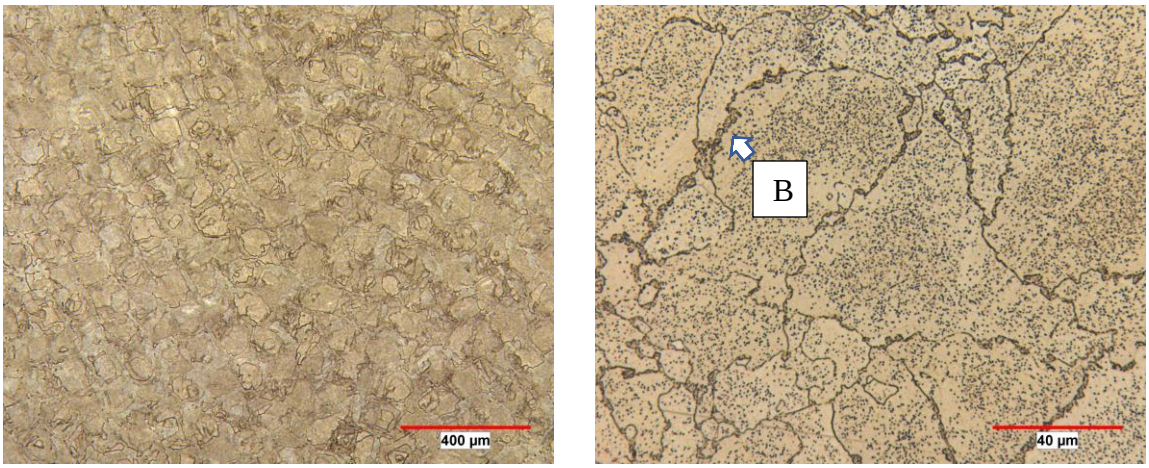

Figure 7: Optical micrographs of the FSLA alloy heat treated at 850 ^{o}C for 1 hour then furnace cooled. Higher magnification on right shows bainite (B) along grain boundaries.

Heat Treatment (3): This heat treatment was designed to create a martensitic structure using gas quenching. It was determined in the development of the MBJ-FSLA that, although heating to 1200 ^{o}C the alloy transforms completely to austenite, it does not give the time scale for which this transformation will occur. When the alloy is heated into the austenitic region, the alloying elements, most notably carbon, chromium, molybdenum, and silicon need to partition or diffuse from the existing phases (ferrite and carbides) into the forming austenite. Carbon, which diffuses interstitially, has the biggest influence, since it has the greatest mobility and is the most effective element in hardening the martensite. The work done on the MBJ version of FSLA showed the time scale to accomplish this was about 5 hours. Holding at 1200 ^{o}C for 5 hours and then gas quenching (1.9 ^{o}C per sec) led to a substantial increase in both UTS (726 MPa) and apparent hardness (HRA = 51) when compared to the previous heat treatment. Due to the carbon diffusion into the austenite, the number and size of the carbides were reduced but the transformation product in this case was a mixture of bainite and martensite (Figure 8).

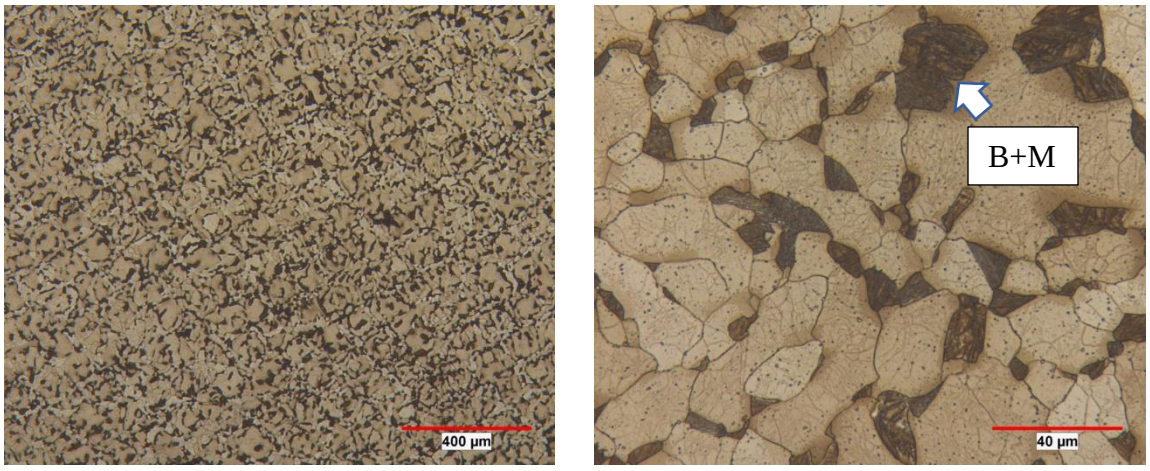

Figure 8: Optical micrographs of the FSLA alloy heat treated at 1200 ^{o}C for 5 hours then gas quenched. Higher magnification on right shows bainite and martensite (B+M).

The transformation phase was more defined forming individual grains as opposed to merely being situated at the grain boundaries.

Heat Treatment (4): The last heat treatment was to austenitize at 1200 ^{o}C for 5 hours, same as the previous heat treatment, but the samples were then quenched in water. This led to a faster cooling rate and the microstructure is shown in Figure 9. The structure achieved was an extremely fine lath martensite (50 vol.%) and ferrite with carbides, which led to the ultimate tensile strength reaching 925 MPa and an apparent hardness of 56 HRA. The level of carbides located within the ferrite is reduced compared to other heat treatments, because the carbon has had time to diffuse into the austenite becoming trapped within the martensite during the rapid cooling. This cooling rate does not allow the carbon to be available for the formation of carbides. Further refinement of the mechanical properties and hardness can be achieved by tempering the microstructure from the quenched condition.

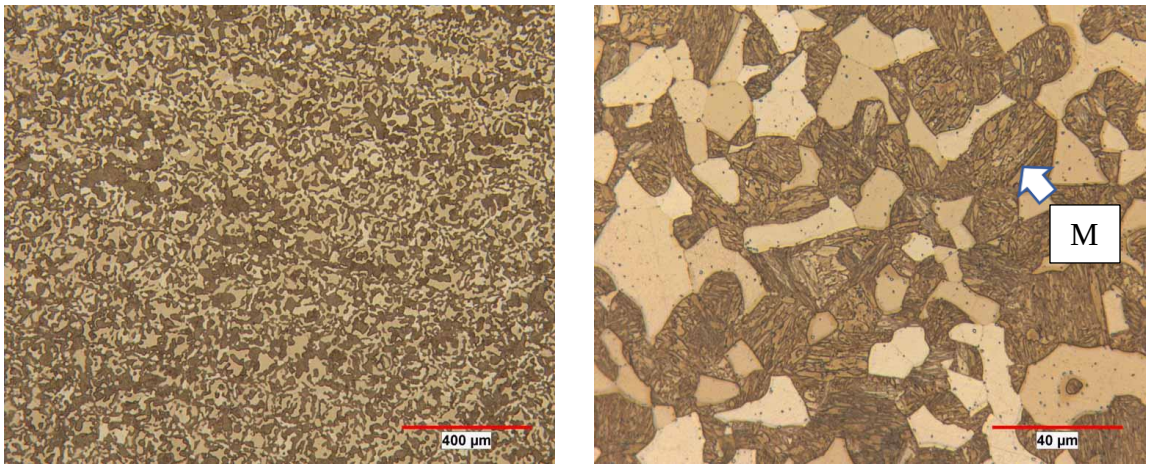

Figure 9: Optical micrographs of the FSLA alloy heat treated at 1200 ^{o}C for 5 hours then water quenched. Higher magnification on right shows martensite (M).

When all mechanical properties of the heat treatments discussed are compared to the wrought version of DP Steels and the FSLA printed by MBJ one can see that, due to the higher density of laser printed samples (>99.9% versus 97.5% for MBJ), the ductility at any given ultimate tensile strength is higher for the samples printed by LPBF (Figure 10). In addition, the mechanical properties of the LPBF-FSLA are superior to the wrought grades of dual phase steels. Since the range of properties can be achieved with one powder the development of the printer settings can be reduced allowing the end user to utilize one powder for a wide range of mechanical property requirements.

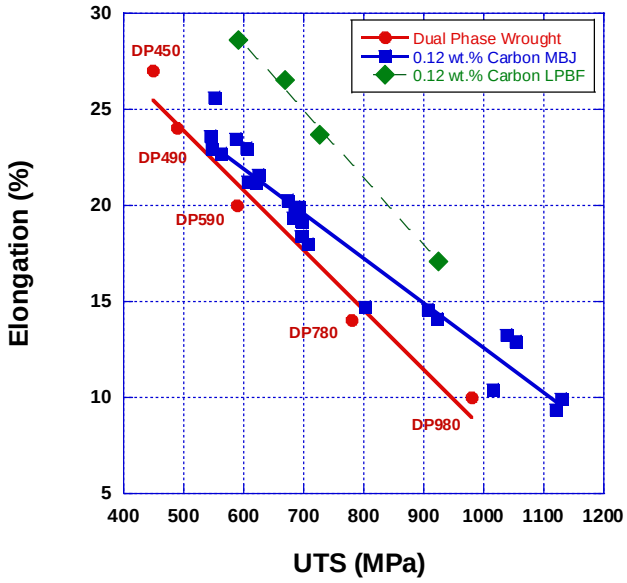

Figure 10: Mechanical Properties of Laser FSLA compared to wrought Dual Phase Steels and FSLA printed by MBJ.

As discussed previously the chemical composition of the FSLA alloy was designed primarily to enhance sintering during the binder jet process. In a previous paper, it was detailed, that to maximize the sinterability of the alloy, the alloy had an equal mixture of ferrite and austenite at the sintering temperature. The increased grain boundary area that was generated by this balanced microstructure led to increased diffusion and better sinterability of the alloy. Control of the phase proportions was developed by adjusting the austenite stabilizers (carbon) and ferrite stabilizing elements (chromium, molybdenum, and silicon). Since carbon is such a strong austenite stabilizer, it was limited to approximately 0.12 wt.% in the MBJ composition. If the carbon content were significantly greater than this level, a high percentage of austenite would have been formed at the sintering temperature and reduced the achievable sintered density. However, with LPBF, the carbon level can be increased since the material is being melted and not sintered. It is typically recognized that a carbon level of approximately 0.20 wt.% can successfully be processed by LPBF without the tendency to crack due to the formation of martensite. Therefore, it was decided to produce a higher carbon version of the FSLA.

Recognizing the powder producer's desire to maximize the utilization of the powder particle size distribution available from one atomizing run, it was decided to take the lower carbon material that was developed for MBJ, in the particle size range of 15-53 μm and increase the carbon content by a common PM processing method called Distaloying.[14] In the distaloy process, alloying elements like molybdenum and nickel, and in this case carbon, in the form of powders can be mixed with the base alloy (FSLA) and then heated under a hydrogen atmosphere at a temperature where the alloying elements diffuse into the base powder, thus making a homogenous powder alloy. In this regard, it

allows more flexibility in utilizing the other particle size distributions for other AM processes.

For this study, a FSLA powder initially containing 0.12 wt.% carbon, was increased to a carbon level of 0.18 wt.% by mixing the FSLA powder with a fine graphite powder and heating under a hydrogen atmosphere at a temperature of 950 ^{o}C. Previous studies have shown graphite goes into solution in iron between 700 and 800 ^{o}C.[15] This powder was printed utilizing the same printer settings as the 0.12 wt.% carbon alloy described previously. The material was given the same heat treatments with the expectation that the higher carbon levels would lead to an increased level of transformation products (bainite and martensite). This in turn, would lead to an increased level of mechanical properties, specifically ultimate tensile strength. The results of the heat treatments are as follows:

Heat Treatment (0)- Table III shows the mechanical properties of the FSLA at the higher level of carbon (0.18 wt.% versus the 0.12 wt.% in Table II). Heat Treatment Zero (0) is in the as built condition. Since the FSLA carbon level is now higher, there is an increase in the amount of transformation product that occurs during cooling from the melt temperature (Figure 11). Qualitative image analysis was used to determine the structure contained 52% fraction of transformation product with the balance being ferrite with carbides. Unlike the lower carbon level in which the transformation product was bainite, the transformation product in this case is predominantly martensite. This led to a substantial increase in UTS and apparent hardness in the higher carbon version of FSLA. Further changes in microstructure were seen since more carbon remained in the austenite, and consequently in the transformed martensite, eliminating the precipitated carbides at the grain boundaries that were present at the lower carbon level.

Table III: Mechanical properties of FSLA-LPBF (containing 0.18 wt.%) for various heat treatments.

Heat Treat #	Condition	UTS [MPa]	0.2%YS [MPa]	Elong [%]	Hardness [HRA]
0	As Built	1057	888	18.2	62
1	1200 ^{o}C 1hr / 800 ^{o}C 2hr	676	407	24.2	48
2	IA 850 ^{o}C Furnace Cool	800	607	22.5	57
3	IA 1200 ^{o}C 1 hr Gas Quench	1130	655	12.9	64
4	IA 1200 ^{o}C Water Quench	1398	1099	14.8	70

Table III shows the UTS in the as built condition is 1057 MPa with an apparent hardness of HRA 62. The ductility of the alloy is quite high (> 18%) when compared with the lower carbon version (0.12 wt.%) due to the absence of precipitated grain boundary carbides. The increase in carbon content had the desired effect of increasing the hardenability of the alloy. Despite the higher carbon levels, all specimens used for this heat treatment and subsequent heat treatments were crack free and achieved the high density of the lower carbon FSLA (>99.9%).

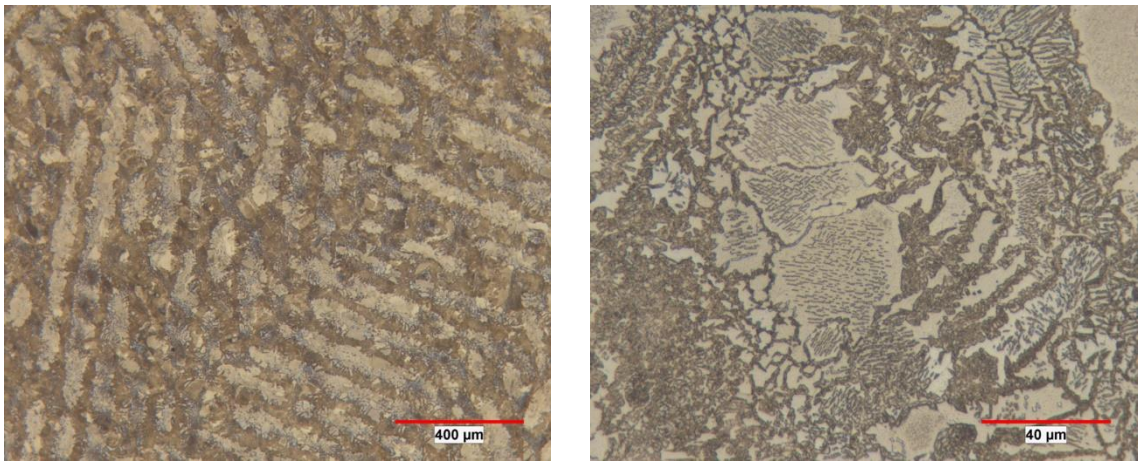

Figure 11: Optical micrographs of the FSLA in the as printed condition with 0.18 wt.% carbon.

Heat Treatment (1)- As a reminder, this heat treatment was designed to provide the maximum amount of ferrite to develop a steel with the highest amount of ductility. The microstructure of the FSLA had a volume fraction of ferrite of 95% with a small percentage of lath martensite that formed during cooling. The martensite in this case may have formed due to the gas quenching. At the 0.18 wt.% carbon level, this cooling rate may have been enough to transform the austenite to martensite as the hardenability of the 0.18 wt.% carbon version of the FSLA would be greater than the 0.12 wt.% version (Figure 12). The UTS and yield strength increased with carbon level, with the ductility not significantly impacted (Table III).

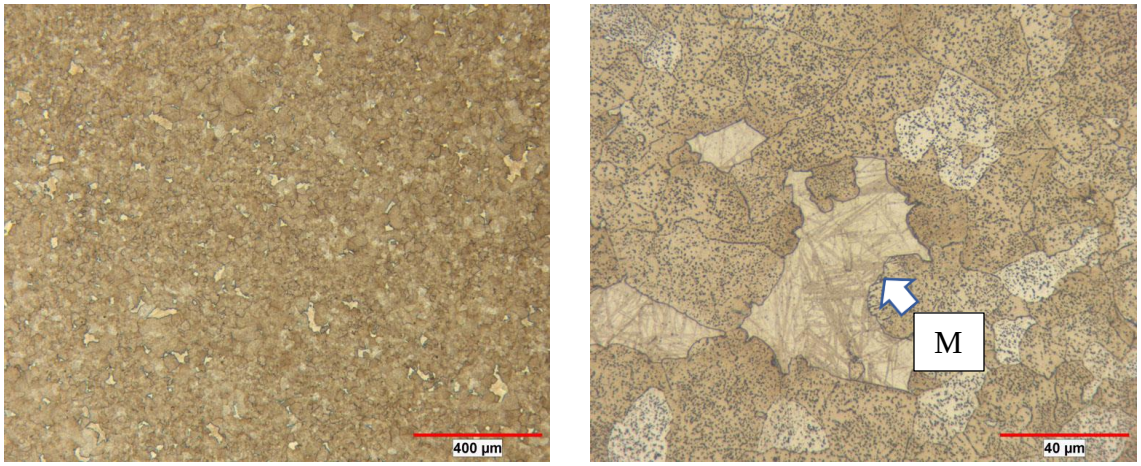

Figure 12: Optical micrographs of the FSLA alloy heat treated at 1200 ^{o}C for 1 hour then furnace cooled and held at 850 ^{o}C for 2 hours to maximize the ferrite content. Carbon level 0.18 wt.%. Higher magnification on right shows martensite islands (M).

Heat Treatment (2)- When compared to the same heat treatment at lower carbon (Figure 5) the banding between the transformation product and the ferrite is quite evident in the lower magnification micrograph of Figure 13. When examined at higher magnifications, the ferrite grains are extremely fine in certain areas while in other areas the ferrite grains are coarse. The transformation product in this case appears to be martensite which is just starting to form along

grain boundaries. Due to the presence of martensite, this higher carbon version of the LPBF-FSLA has increased tensile and yield strength and hardness compared with the lower carbon version (Table II).

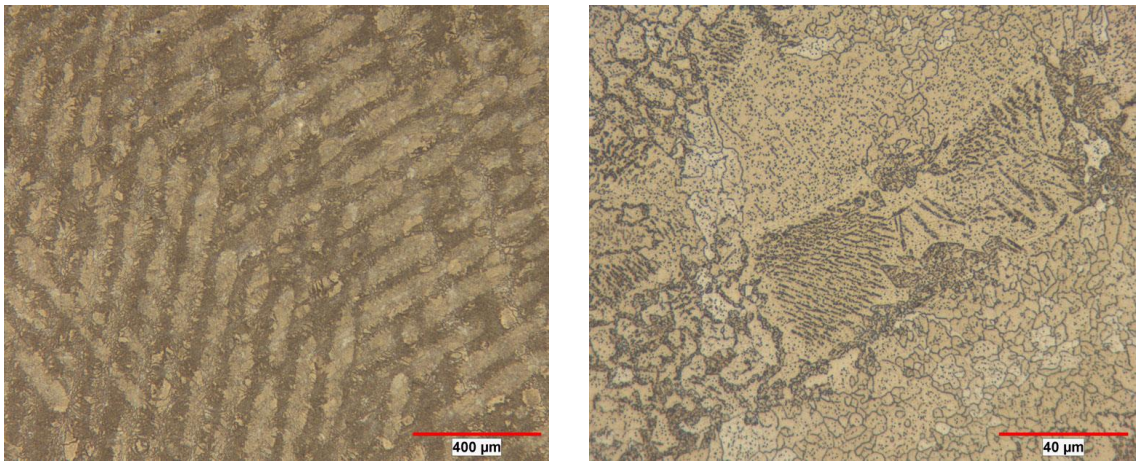

Figure 13: Optical micrographs of the 0.18 wt.% FSLA alloy heat treated at 850 ^{o}C for 1 hour then furnace cooled.

Heat Treatment (3)- Utilizing a heat treatment of holding at 1200 ^{o}C for 5 hours and then gas quenching (1.9 ^{o}C per sec) for the LPBF samples led to a substantial increase in both UTS (up to 1130 MPa) and apparent hardness (HRA = 64) when compared to the 0.12 wt.% carbon version of the FSLA. Due to the carbon diffusion to the transformation products, the number and size of the carbides were reduced in the ferrite (Figure 14). The transformation product in this case was upper bainite (65%) and indicated that a faster cooling rate was required to form martensite.

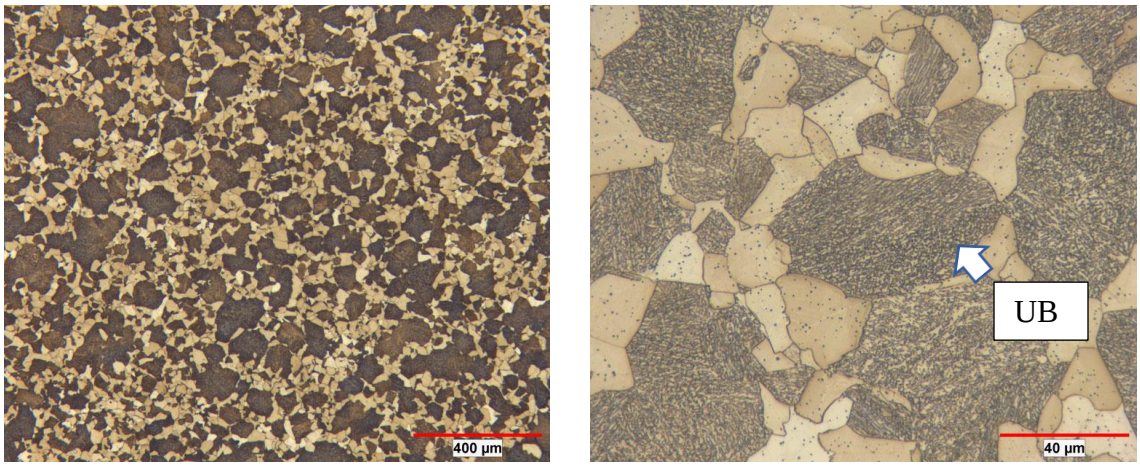

Figure 14: Optical micrographs of the 0.18 wt.% FSLA alloy heat treated at 1200 ^{o}C for 5 hours then gas quenched. Higher magnification on right shows upper bainite (B).

Heat Treatment (4)- The last heat treatment was to austenitize at 1200 ^{o}C for 5 hours, same as the previous heat treatment, but the samples were then quenched in water. This led to a faster

cooling rate and the microstructures shown in Figure 15. The structure achieved was an extremely fine lath martensite which resulted in an ultimate tensile strength reaching approximately 1400 MPa and an apparent hardness of 70 HRA. Further refinement of the mechanical properties and hardness can be achieved by tempering the material.

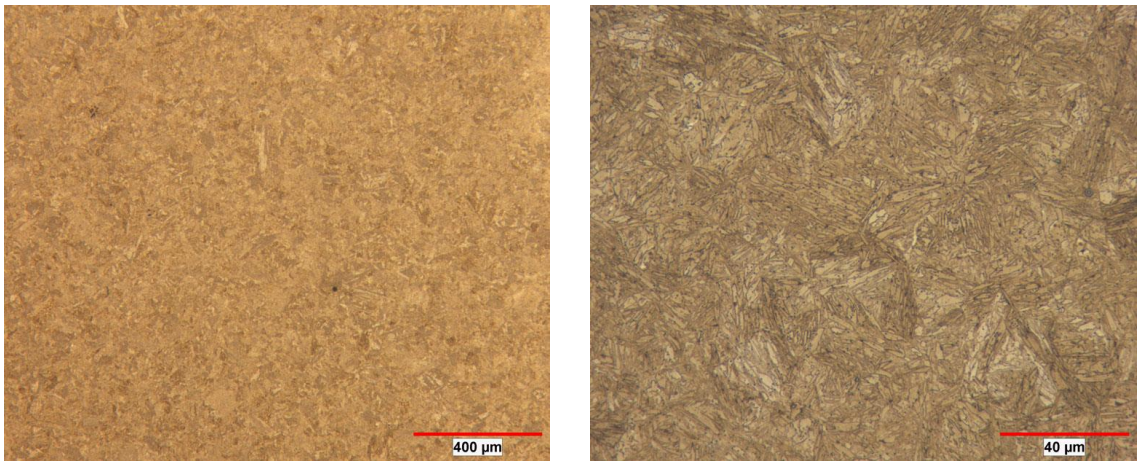

Figure 15. Optical micrographs of the 0.18 wt.% FSLA alloy heat treated at 1200 ^{o}C for 5 hours then water quenched.

The properties from LPBF printed FSLA at the two different carbon levels (0.12 and 0.18 wt.%) are compared to the wrought versions of DP grades and FSLA produced by MBJ in Figure 16. When compared to MBJ processing, the LPBF strength and elongation are superior, even when considering the same carbon level. This is due to the reduced porosity in the LPBF samples (> 99.9%) versus the MBJ samples (97.5%). The additional carbon (0.18 wt.% versus 0.12 wt.%) also increases the range of UTS that can be achieved by the LPBF-FSLA. When compared to the wrought grades of DP steels, the range of properties the LPBF-FSLA exhibits is far superior and for a given UTS, the FSLA has a significant advantage in ductility.

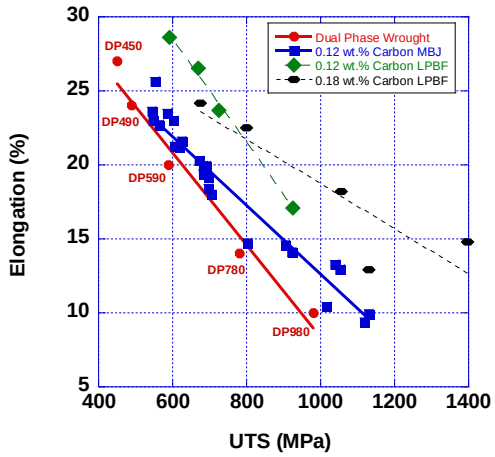

Fig. 16: Mechanical properties of FSLA after different heat treatments. Includes MBJ, LBPF at 0.12 and 0.18 wt.% carbon and wrought grades of Dual Phase Steels.

SUMMARY AND CONCLUSIONS

The use of FSLA powder now has been extended to include LPBF. For the powder producer, this allows an increase in the potential yield of the powder if applications for its use can be determined. It is apparent from this discussion that the LPBF-FSLA properties can be varied significantly by the way the material is heat treated after printing. The wide range of microstructures (transformation products and ferrite) that can be achieved by changing the intercritical annealing temperature, cooling rate, and carbon levels leads to higher strength and elongation combinations than possible by the wrought DP steels. For the additive parts manufacturer, having one material that covers a range of properties is beneficial as the print parameters for the laser printer and the powder behavior in the printer are the same. Additionally, knowledge about how to design the build can be transferred from part to part increasing the speed at which products can be brought to market. The mechanical properties of the LPBF-FSLA are shown schematically in Figure 17 along with available wrought steel grades. The range of product applications of this low alloy steel allow for its potential use in both automotive and industrial applications.

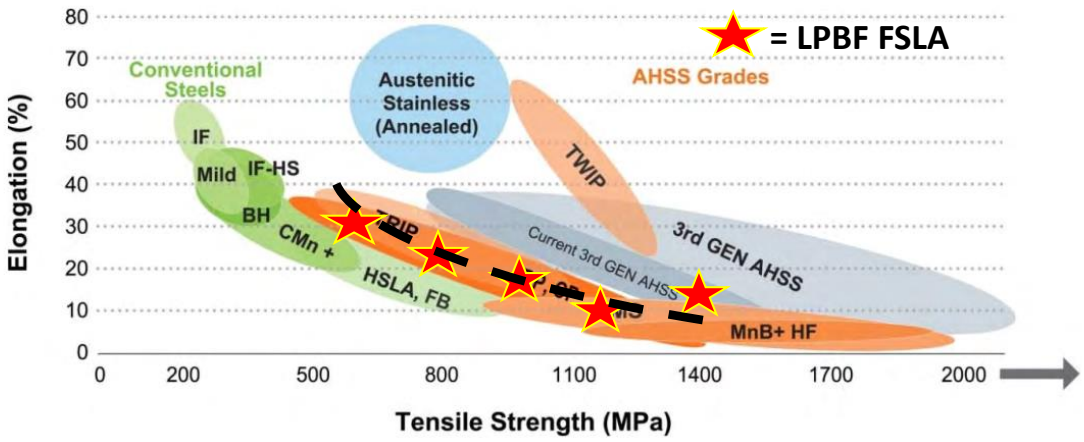

Figure 17: Steel Strength Ductility Diagram, illustrating the range of properties available: wrought steel grades with the addition of the LPBF-FSLA (indicated by stars).[16]

REFERENCES

1. *Materials Standards for PM Structural Parts*, 2020, Metal Powder Industries Federation, Princeton, NJ.
2. *Materials Standards for Metal Injected Molded Parts*, 2018, Metal Powder Industries Federation, Princeton, NJ.
3. C. Schade, T. Murphy, K. Horvay, A. Lawley and R. Doherty, "Development of a Free Sintering Low Alloy (FSLA) Steel for the Binder jet Process," *Advances in Additive Manufacturing with Powder Metallurgy – 2021*, compiled by S. Atre and S. Jackson, Metal Powder Industries Federation, Princeton, NJ, 2021, part 7, pp.287-306.

4. C. Schade, T. Murphy, and K. Horvay, “Microstructure and Mechanical Properties of FSLA Steel Produced by the Binder Jet Process,” *Proceedings of the 2022 Additive Manufacturing with Powder Metallurgy Conference*, compiled by A. Bose and J. Sears, Metal Powder Industries Federation, Princeton, NJ, 2022, part 6, pp. 343-355.
5. L. Donoho, D, Webster, T. Murphy, and C. Schade, “Microstructure and Mechanical Properties of FSLA Steel Produced by the Metal Injection Molding,” *Advances in Powder Metallurgy and Particulate Materials*, compiled by P. Hauck and T. McCabe, Metal Powder Industries Federation, Princeton, NJ, 2022, part 4, pp. 169-180.
6. DP600 Product Datasheet from Salzgitter Flachstahl, Edition 07/10 page 1.
7. M.K. Singh, Application of Steel in Automotive Industry, Int. J. Emergin Technol. Adv. Eng. 6 (2016) 246–253.
8. C.C. Tasan, M. Diehl, D. Yan, M. Bechtold, F. Roters, L. Schemmann, C. Zheng, N. Peranio, D. Ponge, M. Koyama, K. Tsuzaki, D. Raabe, An Overview of Dual-Phase Steels: Advances in Microstructure-Oriented Processing and Micromechanically Guided Design, Annu. Rev. Mater. Res. 45 (2015) 391–431.
9. R.A. Kot and B.L. Bramfit, Editors, “Fundamentals of Dual Phase Steel,” The Metallurgical Society of AIME, 1981.
10. Voest Alpine Product Data Sheet for Dual Phase Steels, June 2019, page 3. https://www.voestalpine.com/stahl/en/content/
11. N.B. Shaw and R.W.K. Honeycombe, “Some Factors Influencing the Sintering Behavior of Austenitic Stainless Steels,” Powder Metallurgy, 1977; vol. 20: pp. 191-198.
12. R.I. Sands and J.F. Watkinson, “Sintered Stainless Steels I.- The Influence of Alloy Composition upon Compacting and Sintering Behavior,” Powder Metallurgy, 1960, No. 5, pp.85-104.
13. *Standard Test Methods for Metals Powders and Powder Metallurgy Products*, Metal Powders Industry Federation, Princeton, NJ,2019.
14. P. Lindskog, “The History of Distaloy,” Powder Metallurgy, 2013; vol. 56, no. 5: pp. 351-361.
15. F. Semel, “Processing Determining the Dimensional Change of PM Steels,” *Advances in Additive Manufacturing with Powder Metallurgy – 2001*, compiled by W.B. Eisen and S. Kassam, Metal Powder Industries Federation, Princeton, NJ, 2001, part 5, pp.113-135.
16. World Steel Auto: http:\\www.worldautosteel.org/